

Electron correlation from path resummations: the double-excitation star

Alex J. W. Thom,* George H. Booth, and Ali Alavi†

University of Cambridge, Chemistry Department, Lensfield Road, Cambridge CB2 1EW, U. K.

(Dated: November 12, 2007)

Resummation over a selected subset of paths allows the approximate evaluation of a N -electron path-integral. In particular, we show that the double excitation star graph, consisting of all doubly excited determinants attached to the reference Hartree–Fock determinant, has an energy which is easily calculated in $\mathcal{O}[N^4]$ time after integral precomputation, and produces binding curves of a similar quality to CCSD theory for a range of systems including the N_2 molecule, the hydrogen-bonded water dimer, and dispersion dominated Ne_2 and Ar_2 dimers.

I. INTRODUCTION

The calculation of the electronic correlation energy of a molecule is fundamental for an accurate description of inter- and intra-molecular interactions. The usual wavefunction-based approaches are based on many-body perturbation theory or Coupled-Cluster theory. However, the path-integral formulation of quantum mechanics does provide an alternative route to the correlation problem, the exploration of which may yield new approximations and insights. In a previous paper¹, we formulated a method of calculating correlated electronic energies as a discrete path integral in Slater determinant space. This was expressed as a sum over ‘graphs’ of determinants, which themselves sum together exponentially many paths which traverse exclusively the determinants in the graph. In this paper, we concentrate on the case of the star graph, whose form allows its weight to be calculated relatively simply.

II. THEORY

Given a system with Hamiltonian \hat{H} , and a set of orthonormal one-particle spin-orbitals (e.g. Hartree–Fock (HF) orbitals), in the space of Slater Determinants, D_i, D_j, \dots constructed out of these orbitals, we may write the quantities: (using the notation of Ref. 1),

$$w_i = \langle D_i | e^{-\beta \hat{H}} | D_i \rangle \quad (2.1)$$

$$\tilde{E}_i = \frac{\langle D_i | \hat{H} e^{-\beta \hat{H}} | D_i \rangle}{w_i} = -\frac{\partial \ln w_i}{\partial \beta} \quad (2.2)$$

at inverse temperature $\beta = (kT)^{-1}$. In the limit of $\beta \rightarrow \infty$, $\tilde{E}_i \rightarrow E_0$, the ground state energy of the system if D_i has an overlap with the ground state. This can usually be ensured by choosing D_i to be the HF determinant, as we have done in this paper. The quantity w_i can be expanded as a discrete path-integral using the identity $e^{-\beta H} = (e^{-\beta H/P})^P$ for any integer P :

$$w_i = \sum_j \sum_k \dots \sum_l \rho_{ij} \rho_{jk} \dots \rho_{li} \quad (2.3)$$

where $\rho_{ij} = \langle D_i | e^{-\frac{\beta}{P} \hat{H}} | D_j \rangle$ is an element of the high-temperature density-matrix. Eq.(2.3) has a simple in-

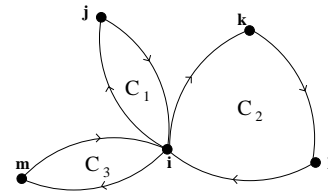


FIG. 1: A star-graph rooted at i . Three cycles, C_1, C_2 , and C_3 are attached together at i .

terpretation: it is the sum over all paths of length P which start and terminate at D_i , the summand being the Boltzmann weight of that path: e.g. for a closed path $i \rightarrow j \rightarrow k \rightarrow \dots \rightarrow l \rightarrow i$, this weight is $\rho_{ij} \rho_{jk} \dots \rho_{li}$. The total path length, P , is chosen such that β/P is small and so ρ elements may be calculated by applying the Trotter formula and a simple Taylor expansion.

Of course the exact evaluation of Eq.(2.3) is a formidable task in all but the simplest cases. Here we propose an approximation to w_i by summing over a subset of paths contained in Eq.(2.3), which consist of distinct cycles attached to i . The set of all such paths are constructable on a simple graph called a ‘star-graph’. An example of a star-graph, with three cycles attached to i (the root of the graph) is given in Fig. 1. In this graph, there are two 2-cycles (labelled C_1 and C_3), consisting of the path $i \rightarrow j \rightarrow i$ and $i \rightarrow m \rightarrow i$, respectively, and a 3-cycle C_2 , consisting of the path $i \rightarrow k \rightarrow l \rightarrow i$. For each such cycle, we define a cycle-function as follows:

$$A_{C_1}(z) = \frac{\rho_{ij} \rho_{ji}}{(z\rho_{ii} - \rho_{ii})(z\rho_{ii} - \rho_{jj})} \quad (2.4)$$

$$A_{C_2}(z) = \frac{\rho_{ik} \rho_{kl} \rho_{li}}{(z\rho_{ii} - \rho_{ii})(z\rho_{ii} - \rho_{kk})(z\rho_{ii} - \rho_{ll})} \quad (2.5)$$

having a numerator containing the product of transition matrix elements defining the cycle, and denominator which is a factorized polynomial of the complex-variable z and the diagonal matrix elements of ρ .

In Refs. 1 and 2, we showed that the weight for a star-graph consisting of an arbitrary number N_C of attached cycles, can be expressed as a contour-integral:

$$w_i = \frac{\rho_{ii}^P}{2\pi i} \oint_C dz \frac{z^P - 1}{z - 1} \frac{1}{1 - \sum_j^{N_C} A_{C_j}(z)}. \quad (2.6)$$

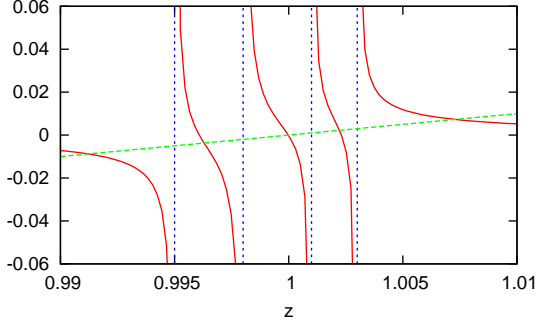


FIG. 2: The graphical solution to Eq. (2.7) by means of the intersection of $z - 1$ (long dashes) with the remainder of Eq. (2.7). The vertical short dotted lines are the poles of the denominator, which bound the roots of the polynomial.

This may be evaluated by determining the roots of its denominator (a polynomial in z) and using the residue theorem. In general this is a tedious task. However, in the case in which we restrict all the cycles of the star to be 2-cycles, i.e. cycles with only one vertex other than \mathbf{i} , a remarkable simplification occurs. In this case, each has a cycle-factor as given in Eq.(2.4) and the denominator polynomial then becomes:

$$\rho_{ii}(z - 1) - \sum_{\mathbf{j}} \frac{\rho_{ij}\rho_{ji}}{(z\rho_{ii} - \rho_{jj})} = 0. \quad (2.7)$$

The roots of this polynomial are bounded by the poles in the denominator (see Fig. 2), and so all can be easily obtained via a Newton-Raphson method. With all the roots, we may factorize the polynomial and evaluate the weight, $w_{\mathbf{i}}$, of the star graph, and from this an energy estimator for the system.

An equivalent, yet simpler, derivation of this result can be seen by recasting Eq. (2.6) in terms of matrices. It can be shown³ that this equation can be rewritten as

$$w_{\mathbf{i}} = \frac{1}{2\pi i} \oint_C dz z^P \frac{|z\mathbf{I} - \rho[\mathbf{j} \dots \mathbf{l}]|}{|z\mathbf{I} - \rho[\mathbf{i} \mathbf{j} \dots \mathbf{l}]|} \quad (2.8)$$

$$= \frac{1}{2\pi i} \oint_C dz z^P [z\mathbf{I} - \rho[\mathbf{i} \mathbf{j} \dots \mathbf{l}]]_{ii}^{-1}, \quad (2.9)$$

where the matrix $\rho[\mathbf{i} \mathbf{j} \dots \mathbf{l}]$ has its rows and columns labelled by the determinants in the star, starting at the root, and consists of all matrix elements between the root and spokes of the star (the first row and column), as well as the diagonal elements,

$$\rho[\mathbf{i} \mathbf{j} \dots \mathbf{l}] = \begin{pmatrix} \rho_{ii} & \rho_{ij} & \rho_{ik} & \cdots & \rho_{il} \\ \rho_{ji} & \rho_{jj} & 0 & \cdots & 0 \\ \rho_{ki} & 0 & \rho_{kk} & \cdots & 0 \\ \vdots & \vdots & \vdots & \ddots & \vdots \\ \rho_{li} & 0 & 0 & \cdots & \rho_{ll} \end{pmatrix}, \quad (2.10)$$

and $\rho[\mathbf{j} \dots \mathbf{l}]$ is the same matrix with the first row and column removed.

It immediately follows that the weight can be cast in terms of the eigen-values and -vectors, $(r_{\alpha}, \mathbf{v}_{\alpha})$, of the $\rho[\mathbf{i} \mathbf{j} \dots \mathbf{l}]$ (which we will now denote simply by ρ),

$$w_{\mathbf{i}} = \sum_{\alpha} |v_{\alpha i}|^2 r_{\alpha}^P. \quad (2.11)$$

The eigenvalue equation $\rho \mathbf{v}_{\alpha} = r_{\alpha} \mathbf{v}_{\alpha}$, when expanded gives equations

$$\rho_{ii}v_{\alpha i} + \rho_{ij}v_{\alpha j} + \cdots + \rho_{il}v_{\alpha l} = r_{\alpha}v_{\alpha i} \quad (2.12)$$

$$\rho_{ji}v_{\alpha i} + \rho_{jj}v_{\alpha j} = r_{\alpha}v_{\alpha j} \quad (2.13)$$

$$\rho_{ki}v_{\alpha i} + \rho_{kk}v_{\alpha k} = r_{\alpha}v_{\alpha k} \quad etc(2.14)$$

Solving all but the first equation, for $v_{\alpha k}$ etc.,

$$v_{\alpha k} = \frac{\rho_{ki}}{r_{\alpha} - \rho_{kk}} v_{\alpha i}, \quad (2.15)$$

and substituting into Eq. (2.12), we recover Eq. (2.7),

$$(r_{\alpha} - \rho_{ii}) - \frac{\rho_{ij}\rho_{ji}}{r_{\alpha} - \rho_{jj}} - \cdots - \frac{\rho_{il}\rho_{li}}{r_{\alpha} - \rho_{ll}} = 0 \quad (2.16)$$

Care must be taken when dealing with degeneracies, i.e. when $\rho_{kk} = \rho_{ll}$. If there are n degenerate ρ_{kk} , their numerators, $\rho_{ik}\rho_{ki}$, may be added together to produce a single term in the polynomial, which will result in a single root, whose eigenvector can be calculated as above. The remaining $(n - 1)$ roots have eigenvalue $r_{\alpha} = \rho_{kk}$, and $v_{\alpha i} = 0$, with components only within the degenerate set, so can be ignored.

In practice, a Newton-Raphson algorithm quickly locates the highest root of the polynomial as, above the highest pole, the gradient is strictly negative. Such an algorithm can fail when locating the lower roots, which are bounded between successive poles as the gradient may approach zero, so a Regula Falsi algorithm is used, followed by some iterations of Newton-Raphson to refine the root. The tolerance for the root-finding was set to 10^{-15} . For the lower roots, we note that when the coupling to an excited determinant, ρ_{ij} , is very small (e.g. $< 10^{-12}$), there is a root very close to its ρ_{jj} , which causes numerical instability in the evaluation of the eigenvector, as the respective denominator in Eq. (2.16) becomes very small, and known only to low accuracy. Because of the small coupling, however, the contributions of such excitations to $w_{\mathbf{i}}$ and $\tilde{E}_{\mathbf{i}}$ are exceedingly small, and may be safely neglected by rejecting all determinants where $|\rho_{ij}| < \rho_{min}$.

With the eigenvectors and eigenvalues we may also now calculate the energy quantity $\tilde{E}_{\mathbf{i}}$, as

$$w_{\mathbf{i}} \tilde{E}_{\mathbf{i}} = \langle D_{\mathbf{i}} | \hat{H} e^{-\beta \hat{H}} | D_{\mathbf{i}} \rangle \quad (2.17)$$

$$= \sum_{\mathbf{m}} \langle D_{\mathbf{i}} | \hat{H} | D_{\mathbf{m}} \rangle \langle D_{\mathbf{m}} | e^{-\beta \hat{H}} | D_{\mathbf{i}} \rangle \quad (2.18)$$

$$= \sum_{\mathbf{m}} \sum_{\alpha} H_{\mathbf{im}} v_{\alpha m} r_{\alpha}^P v_{\alpha i}^*. \quad (2.19)$$

If we fix β/P as a constant, as the ρ matrix elements are dependent on the ratio β/P , not on β or P alone,

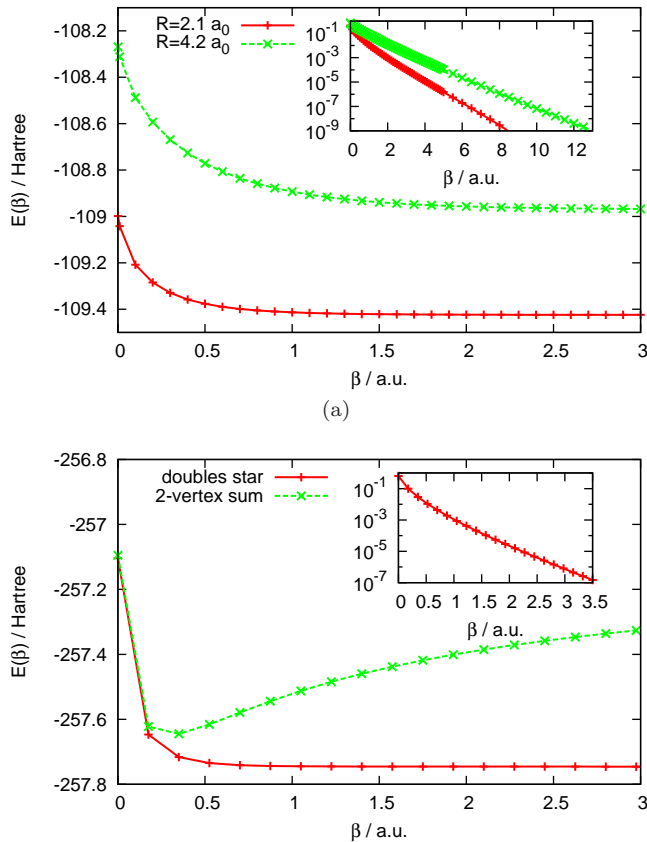


FIG. 3: The convergence of the doubles star energy with β for (a) the N_2 molecule in a cc-pV5Z basis at equilibrium and stretched geometries; and (b) the Ne_2 dimer in an aug-cc-pV5Z basis with bond length $6a_0$. All polynomial roots were used after setting $\rho_{max} = 10^{-9}$. Inset are plots of $E(\beta) - E(\beta = 40)$, showing exponential convergence with β . For Ne_2 , we have included for comparison the energy obtained from summing together all 2-vertex graphs as in Ref. 1. All plots used zeroth order $\rho_{\mathbf{k}\mathbf{k}}^{(0)}$.

and so the eigenvalues r_α are also only dependent on this ratio, and so remain constant. As we approach zero temperature, $\beta \rightarrow \infty$, and consequently for fixed β/P , $P \rightarrow \infty$, and so only the largest eigenvalue contributes to the sums. This renders the calculation of w_i and \tilde{E}_i an $\mathcal{O}[N_{doubles}] \approx \mathcal{O}[N^4]$ process. The convergence of various calculations against β is shown in Fig. 3, and it can be seen that the energy converges exponentially with β , compared to somewhat unphysical dependence of the previous 2-vertex sum formalism¹. From these plots, it is clear that an arbitrarily large value, around $\beta = 40$ is sufficient to ensure only the largest eigenvalue is needed. In all calculations we have fixed the ratio $\beta/P = 10^{-4}$. We note that to accurately calculate the energy for small β , requires *all* the roots of characteristic polynomial to be found, which is computationally very expensive at $\mathcal{O}[N^4 M^4]$. At large β , there is considerable saving in only requiring the highest root.

In applying this procedure to molecular systems, we

have found the behaviour of the resultant energy to be particularly sensitive to the approximations used to calculate the diagonal ρ -matrix elements. Here we present two schemes, both based on the following partitioning of the many-electron Hamiltonian, $\hat{H} = \hat{H}^{(0)} + \hat{H}^{(1)}$, where $\hat{H}^{(0)} = \sum_i \hat{f}(r_i)$, the many-electron Fock operator, and $\hat{H}^{(1)} = \hat{H} - \hat{H}^{(0)}$. We may calculate element $\rho_{\mathbf{j}\mathbf{j}} = \langle D_{\mathbf{j}} | e^{-\frac{\beta}{P} \hat{H}} | D_{\mathbf{j}} \rangle$ by using a Trotter approximation⁴,

$$\begin{aligned} e^{-\frac{\beta}{P} \hat{H}} &= e^{-\frac{\beta}{P} (\hat{H}^{(0)} + \hat{H}^{(1)})} \\ &= e^{-\frac{\beta}{2P} \hat{H}^{(0)}} e^{-\frac{\beta}{P} \hat{H}^{(1)}} e^{-\frac{\beta}{2P} \hat{H}^{(0)}} + \mathcal{O} \left[\left(\frac{\beta}{P} \right)^3 \right] \end{aligned} \quad (2.20)$$

The inner exponential may then be expanded with a Taylor approximation,

$$e^{-\frac{\beta}{P} \hat{H}^{(1)}} = 1 - \frac{\beta}{P} \hat{H}^{(1)} + \mathcal{O} \left[\left(\frac{\beta}{P} \right)^2 \right]. \quad (2.22)$$

We have truncated this approximation at both zeroth, and first order. The zeroth order truncation reduces to sum of the HF energies of the occupied orbitals in a determinant in the exponent,

$$H_{\mathbf{k}\mathbf{k}}^{(0)} = \sum_{i \in \mathbf{k}} \varepsilon_i, \quad (2.23)$$

$$\rho_{\mathbf{k}\mathbf{k}}^{(0)} = \exp \left(-\frac{\beta}{P} H_{\mathbf{k}\mathbf{k}}^{(0)} \right). \quad (2.24)$$

The first-order truncation requires a sum over Coulomb integrals between occupied spin-orbitals,

$$H_{\mathbf{k}\mathbf{k}} = \sum_{i \in \mathbf{k}} h_{ii} + \sum_{\substack{i < j \\ i, j \in \mathbf{k}}} (\langle ij | ij \rangle - \langle ij | ji \rangle) \quad (2.25)$$

$$\rho_{\mathbf{k}\mathbf{k}}^{(1)} = \exp \left(-\frac{\beta}{P} H_{\mathbf{k}\mathbf{k}}^{(0)} \right) \left[1 - \frac{\beta}{P} (H_{\mathbf{k}\mathbf{k}} - H_{\mathbf{k}\mathbf{k}}^{(0)}) \right], \quad (2.26)$$

and is therefore more time-consuming to calculate. The off-diagonal elements begin with first-order terms, so we use this level of truncation throughout:

$$\rho_{\mathbf{k}\mathbf{l}}^{(1)} = -\frac{\beta}{P} \exp \left(-\frac{\beta}{2P} (H_{\mathbf{k}\mathbf{k}}^{(0)} + H_{\mathbf{l}\mathbf{l}}^{(0)}) \right) H_{\mathbf{k}\mathbf{l}}, \quad (2.27)$$

III. APPLICATIONS

We have applied both approximations to two test systems: the N_2 molecule with a cc-pV5Z basis⁷; and the Ne_2 dimer in an aug-cc-pV5Z basis⁸. The nature of the bonding is very different between these two systems, and a description of the dissociation of both of these systems a formidable challenge for a quantum chemical method. DALTON⁹ was used to perform RHF calculations, and the required one- and two-electron integrals were pre-calculated. Dissociation curves are presented in Figs.

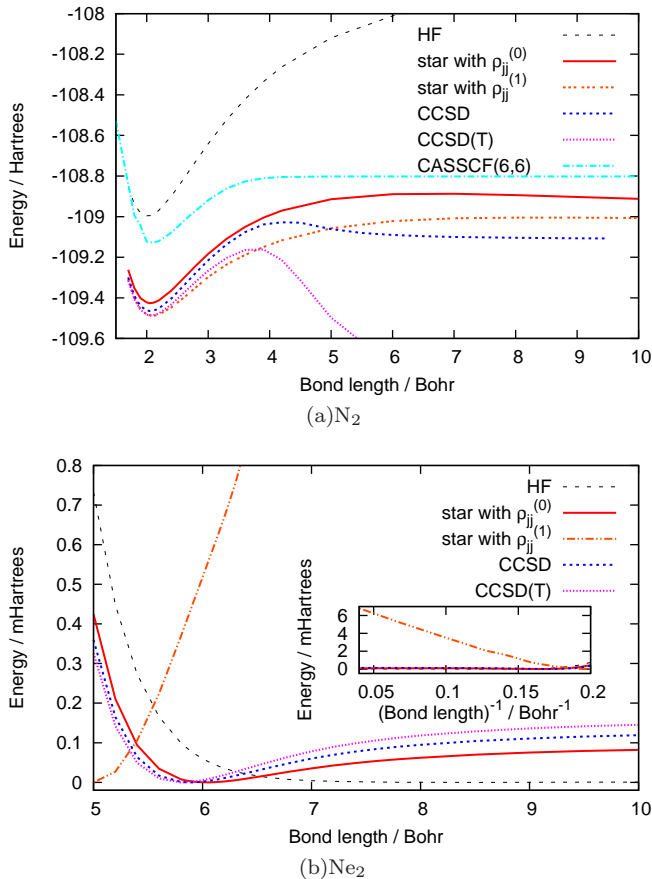


FIG. 4: A comparison of the diagonal Taylor approximations for (a) N_2 in a cc-pV5Z basis; (b) Ne_2 in an aug-cc-pV5Z basis. Results are without counterpoise corrections. The Ne_2 curves have been shifted so their minimum is zero. Inset into (b) is a plot of energy against $1/r$ showing the $1/r$ dependence for the first-order partitioning. Calculations were performed at $\beta = 40$. For N_2 we have also included the CASSCF(6,6) energy, calculated with Gaussian⁵.

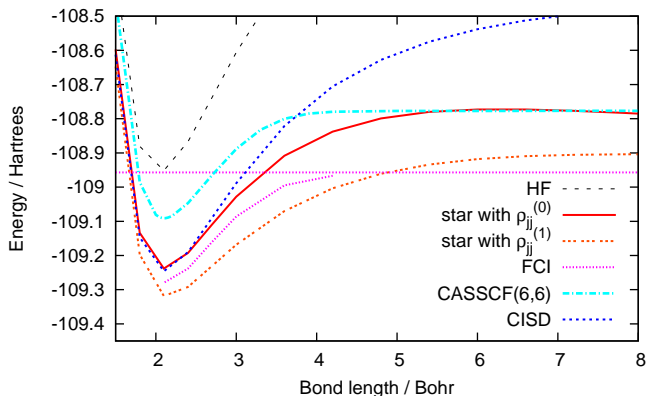


FIG. 5: The frozen-core cc-pVDZ binding curve of N_2 . Doubles-star calculations were performed at $\beta = 40$. FCI calculations were taken from Ref. 6. The horizontal line is the FCI dissociated energy of the molecule, calculated as twice the frozen-core FCI energy of a high-spin single atom.

Method	D_e / eV	r_e / a_0
CASSCF(6,6)	8.906	2.081
MP2	10.396	2.091
CCSD	9.435	2.059
Doubles Star	9.686	2.058
CCSD(T)	9.845	2.073
Experiment	9.911	2.074

TABLE I: The dissociation energies for N_2 in a cc-pV5Z basis, calculated as the difference between equilibrium energy and high-spin separated atoms. MP2, CCSD, and CCSD(T) high-spin results were calculated on single atoms with the Gaussian code⁵ using Unrestricted HF orbitals. The D_e for CASSCF was calculated between equilibrium and $r = 10a_0$. The doubles star high-spin results used atoms $30 a_0$ apart using Restricted HF orbitals. Doubles star calculations were performed at $\beta = 40$.

4(a) and 4(b). It is clear from these figures that the zeroth-order Taylor expansion gives a far better description of the dissociation in both cases without the unphysical $1/r$ tail seen in the first-order approximation. This effect is nonetheless comparatively small, and is swamped by the effects of the bond dissociation in the N_2 plot. We shall return to this in the discussion at the conclusion of this paper. The remaining results have been performed exclusively with the zeroth order partitioning.

Turning to the N_2 molecule, dissociation energies, D_e , and equilibrium bond distances, r_e , are listed in Table I. At stretched bond-lengths, despite the more-physical seeming behaviour of the doubles-star than MP2 and Coupled Cluster theories, there is a pronounced difference between the tail of doubles-star curve and the CASSCF curve. To address this, we have performed calculations using a Dunning cc-pVDZ basis set, and compare against known Full Configuration Interaction (FCI) results⁶ in Fig. 5. This is the largest basis set for which FCI has proved feasible. We note that the tail of the FCI mirrors the CASSCF and decays more quickly than the doubles-star with increasing bond-length. The more accurate FCI and CASSCF description of this tail is known to be due to the inclusion of up-to-hextuple excitations in the calculation. Nevertheless the doubles-star performs considerably better than CISD, which contains contributions from only single and double excitations.

To investigate the intermediate range of bonding strengths, calculations have been performed on the binding curve of the water dimer in an aug-cc-pVDZ basis¹⁰. The geometry as Mas *et al.*¹¹ was used, with varying oxygen-oxygen bond length and results are shown in Fig. 6. The hydrogen bonding in this system seems to be very well described by all the correlation methods used, with the doubles star curve lying between the CCCSD and CCSD(T).

The dissociation curve of the weakly dispersion-bound argon dimer in an aug-cc-pVQZ basis⁸ is shown in Fig. 7. C_6 and C_8 coefficients from Ne_2 and Ar_2 binding curves are shown in Table II. Although the doubles-star does

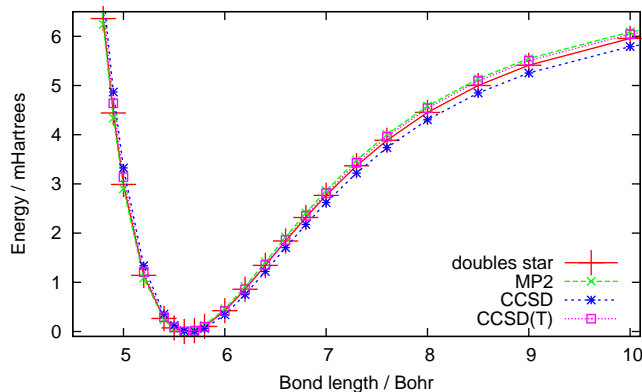


FIG. 6: The counterpoise corrected binding curve of the water dimer in an aug-cc-pVDZ basis, showing the doubles star lying between the CCSD and CCSD(T) curves. All curves have been shifted to place the minimum at zero energy. Calculations were performed at $\beta = 45$.

	Method	$C_6 / \text{Har } a_0^6$	$C_8 / 10^3 \text{ Har } a_0^8$
Ne ₂	MP2	5.56(7)	0.045(5)
	CCSD	5.62(6)	0.064(4)
	Doubles Star	4.48(6)	0.035(4)
	CCSD(T)	6.42(6)	0.077(4)
Ar ₂	MP2	123(10)	-2.2(6)
	CCSD	102(10)	-2.4(6)
	Doubles Star	99(10)	-2.5(6)
	CCSD(T)	112(10)	-2.1(6)

TABLE II: C_6 and C_8 coefficients from a fit of the binding curve tail to $E = -C_6 r^{-6} - C_8 r^{-8} + B$ beginning from $r=8 a_0$. Neon atoms used an aug-cc-pV5Z basis, and argon atoms an aug-cc-pVQZ basis. All energies were counterpoise corrected. Doubles star calculations for Ne had $\beta = 40$, and for Ar had $\beta = 45$.

not capture the full binding energy of the Ar₂ dimer, the C_6 coefficient shows a reasonably close match, suggesting that the method might well be appropriate at capturing non-local, distant dispersion interactions.

As this method requires the same integrals as MP2 theory, and, with the addition of a prefactor for the iterative solution of the equations, the same formal $\mathcal{O}[N^2 M^2]$ scaling, it immediately becomes a competitive correlation method. Absolute timings are shown for a linear chain of neon atoms are shown in Fig. 8. Here we see that the scaling bottleneck is the $\mathcal{O}[N^5]$ integral transformation. The MP2 calculations performed do not use pre-transformed integrals, and the transformation is contracted into the evaluation of the energy. This leads to higher prefactors for the calculation, and it can be seen that the $\mathcal{O}[N^5]$ scaling regime has not yet taken over.

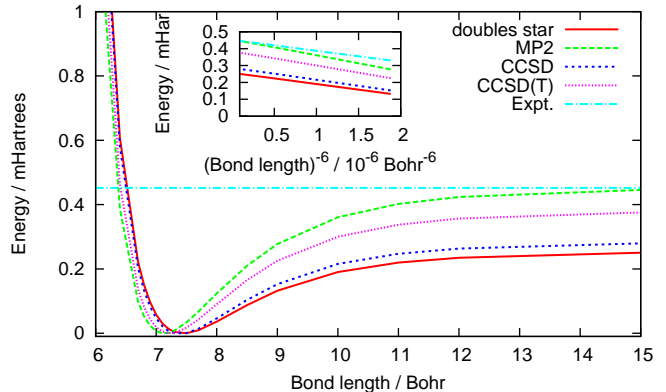


FIG. 7: The counterpoise corrected binding curve of Ar₂ in an aug-cc-pVQZ basis. All curves have been shifted to place the minimum at zero energy. Inset is a plot of the tail of the curve against $1/r^6$, showing a close match between the CCSD and doubles star C_6 coefficients. Calculations were performed at $\beta = 45$. Also shown are the experimental dissociation energy¹² and the C_6 coefficient used in Ref. 13.

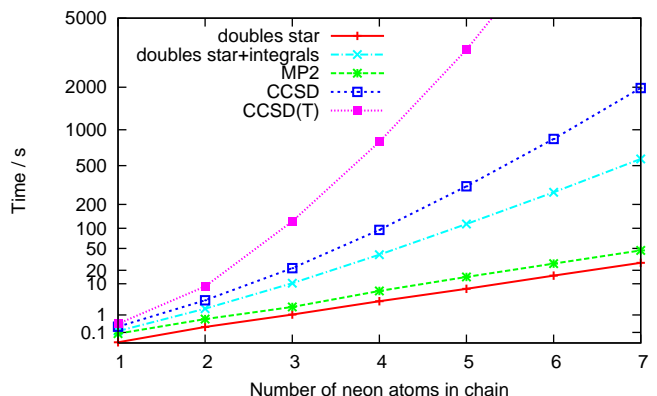


FIG. 8: The CPU time required for calculations on a linear chain of neon atoms, separated by $6 a_0$, in the cc-pVTZ basis set on a Pentium IV. The vertical scale is non-linear and plotted as the fourth root of the time taken.

IV. CONCLUSIONS

Returning to the discussion of the first-order diagonal elements, an investigation on a small basis helium dimer shows that the r^{-1} behaviour is caused by coupling to excited determinants which have a charge-transfer character, and thus a r^{-1} dependence in the value of H_{jj} . Calculations on the full graph for this system, which also includes all connections *between* double excitations do not show this dependence. We may therefore infer that the exclusion of the coupling between double excitations is, by itself, an inconsistent truncation, which may be remedied by using a zeroth-order diagonal matrix elements. These factors will require careful investigation when extending the star to include further excitations and couplings, which will form the basis of a future work.

The results of our new method do appear encouraging. Further development and investigation is warranted. In particular, we would like to understand the reason why using the zeroth-order Taylor expansion for $\rho_{ii}^{(0)}$ works well, but a higher-order expansion for those matrix elements fails, and the connection of this observation with the structure of the 2-vertex star-graph. Furthermore, it will be interesting to see if inclusion of triple excitations into the star-graph leads to similar gains in accuracy that is generally observed with the coupled cluster method in going from CCSD to CCSD(T). Overall, we believe that the double-excitation star method produces binding curves of around a CCSD quality, and has the advantage of requiring the same integrals as and scaling at the same level as MP2 theory. Moreover, unlike MP2 theory, it does not suffer from problems with degeneracies or near-degeneracies, and can therefore be applied to processes such as multiple-bond breaking which lead to divergences in other theories. The doubles-star seems to describe rea-

sonably well the dissociation of the N_2 molecule, which being a triply-bonded system has proven very challenging for single-reference methods. It does not, however, achieve the same quickly decaying tail as FCI, but it is hoped that the inclusion of higher excitations will remedy this.

Furthermore, the current wealth of knowledge of localization methods to reduce the scaling of the integral transformation and MP2 calculation can equally well be applied to the doubles star which raises the tantalizing possibility of linear scaling.

V. ACKNOWLEDGEMENTS

The support of the EPSRC through a Portfolio Award is gratefully acknowledged.

* Electronic address: ajwt3@cam.ac.uk

† Electronic address: asa10@cam.ac.uk

¹ A. J. W. Thom and A. Alavi, *J. Chem. Phys.*, 2005, **123**, 204106–1–13.

² A. Alavi and A. J. W. Thom, *Lect. Notes Phys.*, 2006, **703**, 685–704.

³ A. J. W. Thom *Towards a Quantum Monte Carlo approach based on path resummations* PhD thesis, University of Cambridge, 2006.

⁴ H. F. Trotter, *Proc. Am. Math. Soc.*, 1959, **10**, 545–551.

⁵ M. J. Frisch, G. W. Trucks, H. B. Schlegel, G. E. Scuseria, M. A. Robb, J. R. Cheeseman, J. A. Montgomery, Jr., T. Vreven, K. N. Kudin, J. C. Burant, J. M. Millam, S. S. Iyengar, J. Tomasi, V. Barone, B. Mennucci, M. Cossi, G. Scalmani, N. Rega, G. A. Petersson, H. Nakatsuji, M. Hada, M. Ehara, K. Toyota, R. Fukuda, J. Hasegawa, M. Ishida, T. Nakajima, Y. Honda, O. Kitao, H. Nakai, M. Klene, X. Li, J. E. Knox, H. P. Hratchian, J. B. Cross, V. Bakken, C. Adamo, J. Jaramillo, R. Gomperts, R. E. Stratmann, O. Yazyev, A. J. Austin, R. Cammi, C. Pomelli, J. W. Ochterski, P. Y. Ayala, K. Morokuma, G. A. Voth, P. Salvador, J. J. Dannenberg, V. G. Zakrzewski, S. Dapprich, A. D. Daniels, M. C. Strain, O. Farkas, D. K. Malick, A. D. Rabuck, K. Raghavachari,

J. B. Foresman, J. V. Ortiz, Q. Cui, A. G. Baboul, S. Clifford, J. Cioslowski, B. B. Stefanov, G. Liu, A. Liashenko, P. Piskorz, I. Komaromi, R. L. Martin, D. J. Fox, T. Keith, M. A. Al-Laham, C. Y. Peng, A. Nanayakkara, M. Challacombe, P. M. W. Gill, B. Johnson, W. Chen, M. W. Wong, C. Gonzalez, and J. A. Pople, Gaussian 03, Revision D.01, 2003.

⁶ G. K.-L. Chan, M. Kállay, and J. Gauss, *J. Chem. Phys.*, 2004, **121**, 6110–6116.

⁷ T. H. Dunning, Jr., *J. Chem. Phys.*, 1989, **90**, 1007–1023.

⁸ D. E. Woon and T. H. Dunning, Jr., *J. Chem. Phys.*, 1994, **100**, 2975.

⁹ DALTON, Release 2.0, a molecular electronic structure program, 2005.

¹⁰ R. A. Kendall, T. H. Dunning, Jr., and R. J. Harrison, *J. Chem. Phys.*, 1992, **96**, 6769.

¹¹ E. M. Mas and K. Szalewicz, *J. Chem. Phys.*, 1996, **104**, 7606–7614.

¹² T. Helgaker, P. Jørgensen, and J. Olsen, Wiley, Chichester, 2000; chapter 14.

¹³ K. Patkowski, G. Murdacheaw, C.-M. Fou, and K. Szalewicz, *Mol. Phys.*, 2005, **103**, 2031–2045.